



Fatty acid sources and distributions in typical karst river water and groundwater: Insights from hydrochemistry and microbial traces

Zuobing Liang^{1,3} · Shaoheng Li^{1,2} · Pengcheng Zhang⁵ · Rui Li⁴ · Qirui Wu⁴ · Zaizhi Yang¹ · Di Tian¹ · Kun Ren^{1,6} · Lei Gao⁴ · Jianyao Chen¹

Received: 15 April 2024 / Accepted: 10 October 2025

© The Author(s), under exclusive licence to Springer-Verlag GmbH Germany, part of Springer Nature 2025

Abstract

Dissolved organic matter (DOM) is a vital component of organic material in ecosystems. While DOM dynamics in general watersheds are well-studied, its composition and behavior in karst watersheds remain poorly constrained due to unique hydrogeological complexities. The focus of this study is on the Lianjiang River Basin, which is a typical karst watershed in southern China, and the objective of the study is to identify the sources of fatty acids, analyze the impact of river water-groundwater relationships on the distribution of fatty acids, and investigate the behavior of dissolved organic matter (DOM) in the karst water system. In this study, measurements of fatty acid and dissolved organic carbon (DOC) concentrations, hydrochemical indicators, and stable isotopic compositions (δD and $\delta^{18}O$) were taken for surface water and groundwater samples, including both shallow and deep groundwater. Additionally, microbial analysis was conducted on the groundwater samples to gain further insight into the microbial communities present in the karst water system. Fatty acid contents in river water, shallow groundwater, and deep groundwater were $15,595 \pm 14,164$ ng/L, $15,600 \pm 10,089$ ng/L, and $27,353 \pm 20,378$ ng/L, respectively. The study found that deep groundwater had the highest concentrations of fatty acids, while river water and shallow groundwater had similar fatty acid contents. The higher standard deviation of fatty acids in surface water and groundwater samples can be attributed to the unique characteristics of karst aquifers. Fatty acids in shallow groundwater mainly originate from three sources: surface soil-associated organic matter, fecal-associated sources, and pharmaceutical or cosmetic-associated sources. Hydrochemical and stable isotope compositions (δD and $\delta^{18}O$) showed river water were recharged by adjacent groundwater, which influenced the spatial distribution of fatty acids in the study area. The deep karst aquifer may serve as a DOM sink in the karst watershed, and the DOM in the karst water system was affected by natural and anthropogenic sources input as well as surface water-groundwater relationships during the dry season.

Keywords Fatty acids · Hydrochemistry · Environmental isotope · Karst water system · Lianjiang river watershed

Shaoheng Li contributed equally to this work and should be considered a co-first author.

✉ Zuobing Liang
liangzb@lsbg.cn

¹ School of Geography and Planning, Sun Yat-sen University, Guangzhou 510275, China

² School of Geography and Tourism, Jiaying University, Meizhou 514015, China

³ Jiangxi Provincial Key Laboratory of Carbon Neutrality and Ecosystem Carbon Sink, Lushan Botanical Garden, Jiangxi Province and Chinese Academy of Sciences, Jiujiang 332900, China

⁴ South China Botanical Garden, Chinese Academy of Sciences, Guangzhou 510275, China

⁵ School of Economics and Management, Guangzhou Vocational University of Science and Technology, Guangzhou 510275, China

⁶ Institute of Karst Geology, Key Laboratory of Karst Dynamics, Chinese Academy of Geological Sciences, Ministry of Natural Resources & Guangxi, Guilin 541004, China

Introduction

Dissolved organic matter (DOM) is a crucial and widespread source of organic substances within ecosystems, and its abundance and composition are subject to spatial and temporal variations (Simon et al. 2010). DOM plays a vital role in ecosystems by serving as a primary source of nutrients for organisms dependent on groundwater, as well as acting as a donor and acceptor of protons and electrons in pH buffering and biogeochemical reactions. Additionally, DOM contributes to the hydrodynamics of contaminant transport (Bernhardt and Likens 2002; Cory and McKnight 2005).

In the Earth's continental area karst regions constitute about 7–12% of the total areas, and their groundwater resources, which make up a quarter of the world's freshwater supply, are crucial for the inhabitants of these areas (Hartmann et al., 2014). Karst environments are frequently used for the disposal of solid and liquid wastes from industrial and agricultural activities, which can lead to the contamination of karst groundwater. Due to the potential for contamination from human activities, the critical zone in karst environments is regarded as highly vulnerable to pollution (Green et al. 2019; Worthington et al. 2012). In addition, karst aquifers are characterized by high heterogeneity, which is attributed to transmissive fractures and conduits embedded in a low-density rock matrix (Charlier et al. 2012; Željković et al., 2015). As a result of their high heterogeneity, karst aquifers exhibit a high degree of hydraulic connectivity with the land surface, which can lead to rapid transport of contaminants (Borović et al. 2019; Medici et al. 2021; Sullivan et al. 2019). Karst aquifers, due to their high permeability, are hydrologically connected to surface water, which makes them vulnerable to inputs of dissolved organic matter as well as anthropogenic organic matter from the surface (J Jin et al. 2014). Consequently, the behavior of dissolved organic matter derived from the surface in karst aquifers is primarily regulated by water-rock-microbe interactions that occur on the surface.

DOM's essential role in different biochemical and ecological processes has led to extensive research on its behavior in karst water systems. At the watershed scale, the abundance of DOM is influenced by the dynamic interplay of various sources of DOM and biogeochemical reactions that occur along the flow paths of water as it traverses the landscape (Bernhardt and Likens 2002; Jaffé et al. 2008; Wen Liu et al. 2018a). Although numerous studies have evaluated the characteristics of DOM in karst water systems (Lü et al. 2020; W. Liu et al. 2018b; Quiers et al. 2014; Yao et al. 2014), DOM dynamics in general watersheds are well-studied, its composition and behavior in karst watersheds remain poorly constrained due to unique hydrogeological

complexities or on the ways in which surface water-groundwater interactions can influence DOM properties.

Fatty acids, recognized as one of the typical lipid biomarkers, are valuable tools for identifying the sources of DOM and the biogeochemical processes associated with it. As an example, even-numbered carbon fatty acids (C16:0-C30:0) are primarily derived from vascular plants, and waxy coatings on plant leaves, flowers, and pollen are primarily composed of long-chain fatty acids (Rieley et al. 1991; Yoshinaga et al. 2008; Rielley et al., 1991); the mono-unsaturated fatty acids (MUFA) C18:1 ω 7 is commonly viewed as bacterial biomarkers (Christodoulou et al. 2009); C14:0, C16:0 and C18:0 were reported exclusively in phytoplankton (Napolitano et al. 1997; Wakeham 1985). Fatty acids offer several advantages over other methods for identifying DOM characteristics in aqueous environments. They not only provide reliable information on the major sources of DOM but also enhance our understanding of the associated biogeochemistry. Moreover, they can simultaneously identify a wide spectrum of different sources and exhibit high resolution for mixed DOM sources. In addition, critical biomarkers for tracking DOM sources and microbial processes in aquatic systems, with high sensitivity to anthropogenic inputs (Rieley et al., 1991). Therefore, fatty acids can offer valuable insights into the environmental dynamics of organic matter in diverse ecosystems. Moreover, isotopic tracers ($\delta D/\delta^{18}O$) elucidate water source mixing, while microbial communities provide direct evidence of DOM processing pathways—complementing hydrochemical and biomarker approaches in karst systems.

Our study involved examining the distribution and origin of DOM using fatty acid lipid biomarkers in a typical karst watershed in southern China. To explore the transformation of DOM, we examined the behavior of DOM in both river water and groundwater, as well as the interrelationship between river water and groundwater in the karst watershed. During a field survey, we collected samples to achieve the following objectives: (1) quantify the content of fatty acids and study their spatial distribution characteristics in different water bodies within the karst watershed, (2) identify the sources of fatty acids in shallow groundwater and examine the influence of surface water-groundwater interactions on the distribution of fatty acids in the river water, and (3) characterize DOM in the karst watershed during the dry season.

Material and methods

Study area

The Lianjiang River basin (located between 112°10' E–113°18' E and 24°09' N–25°07' N) covers an area of

10,061 km² in southern China. It has a typical subtropical monsoon climate, characterized by humid conditions and annual rainfall ranging from 1400 to 2200 mm and the mean annual rainfall is 1770 ± 215 mm (SD, $n=30$ years). The mean annual temperature is 19–20 °C, and precipitation predominantly occurs from April to June, with 45–50% of the annual rainfall received during this period. The region experiences a distinct wet season (April–June), during which >45% of annual rainfall occurs. Sampling was conducted in April 2022 to capture baseline conditions with minimal precipitation. The Lianjiang River basin is comprised of a shallow marine carbonate formation, which accounts for over 60% of the total area.

Sample collection, preparation, and analytical procedures

During the dry season (April 2022), although April marks the onset of the rainy period, early April experiences sporadic rainfall (<10% of monthly average), sampling occurred during this low-flow window to minimize transient hydrologic effects. For shallow groundwater: Samples were collected from rural household dug wells (depth ≤ 15 m), representing the phreatic zone directly recharged by surface water infiltration. Deep groundwater: Samples collected from environmental monitoring wells managed by government agencies (depth ≥ 50 m), accessing confined aquifers with minimal surface influence. We collected a total of 4 L of water from the mainstream and tributaries of the Lianjiang River basin, including 11 river water samples, 19 shallow groundwater samples, and 11 deep groundwater samples. Shallow groundwater samples were also collected near surface sample sites (which are not distinguishable on the sampling map; see Fig. 1). More details about the preparation and analytical procedures of water samples are shown in supporting information.

To measure fatty acids, the collected samples were in 4-L pre-combusted (450°C in a muffle furnace for 4.5 h) brown glass bottles and added three drops of saturated HgCl₂ to prevent microbial activity. The dissolved phase (<0.45 μm) was stored in pre-cleaned 4-L brown glass containers with airtight caps. We stored samples at 4°C and analyzed them within 3 days (Sun et al., 2021). For sample extraction, all lipid processing glassware were combusted at 450°C for 4.5 h. Prior to extraction, nonadecanoic acid was added as an indicator for recovery, and extracted fatty acids using a separating funnel with dichloromethane liquid. Then saponified (or base hydrolyzed) the total lipid extracts from DOM samples.

Water samples for cation analysis (K⁺, Na⁺, Mg²⁺ and Ca²⁺) were filtered through 0.22-μm pore-size membrane filters (Millipore, Burlington, MA, USA); samples were acidified to pH<2 immediately after sampling (Liang et al., 2018). Water samples for isotope analysis ($\delta^{18}\text{O}$ and $\delta^2\text{H}$)

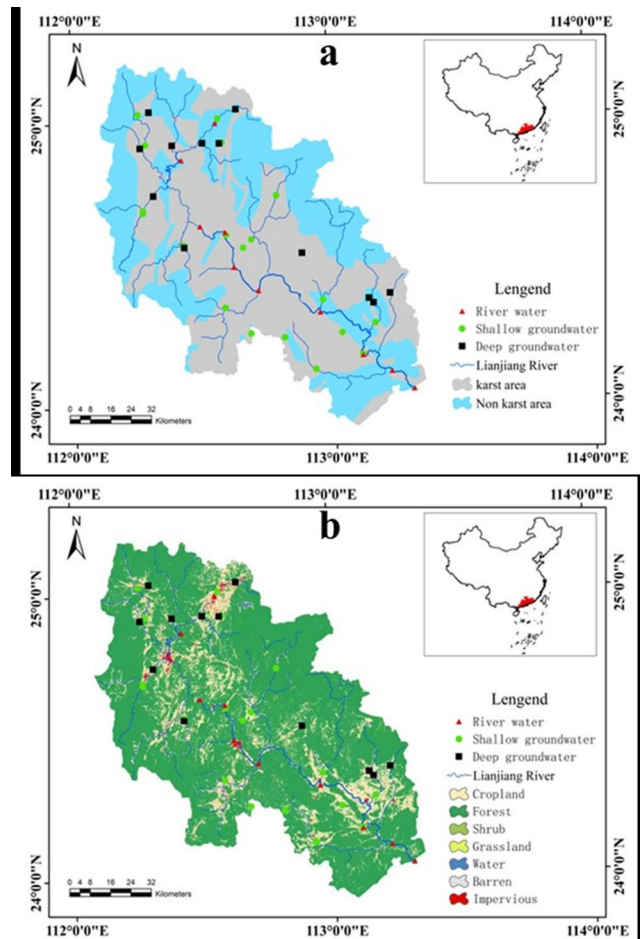


Fig. 1 Characteristics of location, sampling sites, rock (Fig. 1a) and land use types (Fig. 1b) in Lianjiang River watershed

and anions analysis (NO₃⁻, SO₄²⁻ and Cl⁻) were also filtered through 0.22-μm pore-size membrane filters. Water samples for total dissolved organic carbon (DOC) analysis were filtered in-situ through 0.22-μm hydrophilic membrane filters. For microbiological analysis, 2-L water samples were filtered through 0.22-μm pore-size polycarbonate filters. To extract total DNA from water samples, the PowerSoil DNA Isolation Kit (MO BIO Laboratories, Carlsbad, CA, USA) was utilized. After extraction, the quality of the DNA was assessed through agarose gel electrophoresis, and it was subsequently stored at -20 °C. A Qubit® 2.0 fluorometer was used to determine DNA concentrations (Zhu et al., 2020). To ensure accuracy, environmental parameters (pH, electrical conductivity (EC), and temperature) were stabilized and then measured using a multiparameter measurement device (DR/800; HACH, Loveland, CO, USA).

To determine the concentrations of cations (K⁺, Na⁺, Mg²⁺, and Ca²⁺), inductively coupled plasma-atomic emission spectrometry (IRIS-HR, Thermo Jarrel Ash, Franklin, MA, USA) was utilized, with a detection limit of ± 0.05 ppm. An analysis of anions (NO₃⁻, SO₄²⁻, and Cl⁻) was

performed using a DX-600 ion chromatograph (Dionex, Sunnyvale, CA, USA), with a detection limit of ± 0.1 ppm. HCO_3^- was titrated in the field immediately using a portable testing kit (Merck KGaA Co., Darmstadt, Germany), with an accuracy of ± 0.05 mmol/L. The $\delta^{18}\text{O}$ and $\delta^2\text{H}$ values in groundwater were determined using a high-precision laser isotope analyzer (L2130-i Analyzer, Picarro, Santa Clara, CA, USA), with a measurement accuracy of $\pm 0.02\text{‰}$; measurements were reported relative to the Vienna Standard Mean Ocean Water standard. DOC contents were determined by catalytic combustion using a total organic carbon analyzer (TOC-V cph/cpn: Shimadzu Corporation, Kyoto, Japan, with a measurement accuracy of $\pm 2\%$ RSD). Extraction was performed by gas chromatography-mass spectrometry (Agilent 7890 A GC, 5975 C MSD) in the selected ion monitoring mode. Method blanks (solvent) were analyzed, and no interference was observed. Microcosms were constructed, deployed, and analyzed using a modified version of the method of Zhu et al. (2020). In brief, the primer pair 515 F and 806R were used to amplify the V4 region of bacterial 16 S rRNA. The resulting polymerase chain reaction amplicons were sequenced on an Illumina MiSeq platform at Beijing Biomarker Technologies. To obtain effective tags and operational taxonomic units, sequences were analyzed using QIIME and UPARSE software with default settings.

Results and discussion

General hydrogeochemistry of the study area

The range and mean values obtained during sampling campaign of dry season for all parameters included in this study are shown in Table 1. The mean pH values showed no

significant variation from surface water to deep groundwater in the study area ($p > 0.05$). The surface water's EC values ranged from 107.2 $\mu\text{s}/\text{cm}$ to 326.0 $\mu\text{s}/\text{cm}$, with a mean value of 198.8 $\mu\text{s}/\text{cm}$, which was relatively lower compared to other groundwater samples (shallow and deep groundwater). It should be noted that the higher standard deviation value in deep groundwater was due to an abnormal value in one sampling site, with a value of 2109.0 $\mu\text{s}/\text{cm}$, which added to the mean value of EC in deep groundwater. In general, the mean value of EC in shallow groundwater was higher than those in surface water and deep groundwater. Since EC can be used as an index of water quality in areas unaffected by seawater, the higher EC value of shallow groundwater in the study area indicates worse water quality than other water sources (Z Jin et al. 2012; J Li et al. 2017).

The hydrogeochemistry regimes of surface water and groundwater in the Lianjiang River watershed are illustrated in the Piper diagram in Fig. 2. Both surface water and groundwater samples from the Lianjiang River watershed are primarily located on the left side of the diagram, indicating that the primary hydrogeochemical facies is HCO_3^- -Ca, with three samples in the upper part of the diagram representative of the SO_4^{2-} -Ca water type. However, the relative concentration of SO_4^{2-} in shallow groundwater was higher than that in river water and deep groundwater, and this increase is not linked to geological conditions but rather to anthropogenic pressure. Furthermore, the NO_3^- concentrations in most shallow groundwater samples exceed the maximum permissible limit for drinking water according to WHO standards. The higher NO_3^- and SO_4^{2-} concentrations in most shallow groundwater samples suggest anthropogenic pollution resulting from the application of chemical fertilizers and manure in agricultural fields and rural residential areas (Busico et al., 2020; Liang et al., 2018).

Table 1 Descriptive statistics of chemical constituents in the surface water and groundwater

Type	pH	T (°C)	EC ($\mu\text{s}/\text{cm}$)	K^+ (mg/L)	Na^+ (mg/L)	Ca^{2+}	Mg^{2+}	HCO_3^-	Cl^-	SO_4^{2-}	NO_3^-
Surface water ($n=25$)											
Min.	6.2	19.7	107.2	1.0	1.0	15.5	1.7	61.0	1.7	3.8	0.0
Max.	7.7	27.1	326.0	3.2	9.3	50.5	8.3	146.4	6.5	12.1	7.2
Mean	6.9	23.7	198.8	1.7	3.1	34.8	4.1	115.9	3.1	7.8	3.9
SD	0.4	1.6	62.1	0.6	1.9	11.4	1.8	32.5	1.3	2.6	1.3
Shallow groundwater ($n=20$)											
Min.	5.0	19.8	42.6	0.0	0.5	3.2	0.3	42.7	0.8	1.2	0.4
Max.	6.9	25.1	801.0	29.0	26.8	115.0	22.5	359.5	42.8	72.2	229.4
Mean	6.3	22.1	508.2	8.5	14.5	79.4	9.1	240.1	17.6	30.8	49.2
SD	0.4	1.5	159.1	8.1	10.1	21.6	5.8	82.0	11.8	18.6	57.8
Deep groundwater ($n=13$)											
Min.	5.2	19.2	123.6	0.0	1.3	14.5	2.7	61.0	2.0	1.0	0.3
Max.	7.3	24.4	2109.0	5.3	42.8	427.0	82.1	420.9	15.4	2001.6	37.9
Mean	6.6	21.8	583.4	2.2	9.9	113.2	17.6	219.6	6.1	277.2	8.9
SD	0.7	1.7	637.5	1.7	14.0	131.0	26.9	116.8	4.7	700.2	12.8

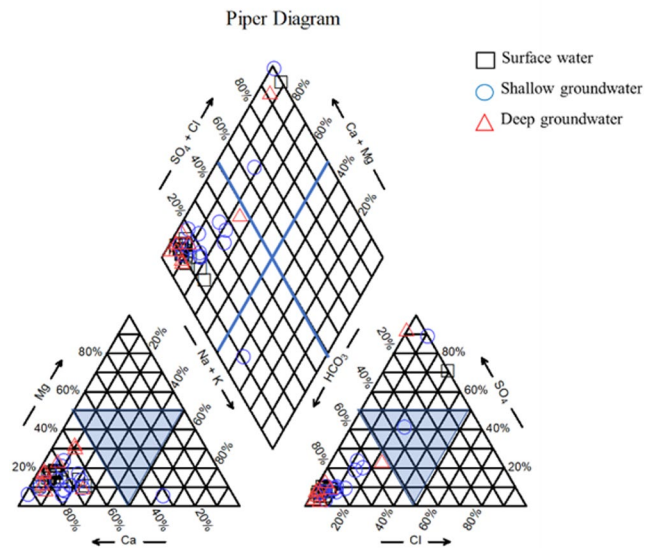


Fig. 2 Piper diagrams for the study areas

Stable isotopic characteristics

Stable water isotopes of oxygen and hydrogen are useful for integrating hydrological process information across different systems (Gat 1996; Z J Li et al. 2019). The δD and $\delta^{18}\text{O}$ values of surface water and groundwater samples are plotted in Fig. 3. As shown in Fig. 3, the δD - $\delta^{18}\text{O}$ values of all studied samples fall on a scatter line around the local meteoric water line (LMWL). The δD - $\delta^{18}\text{O}$ relationships for surface water, shallow groundwater, and deep groundwater were found to be: $\delta D = 4.74\delta^{18}\text{O} - 6.03$ ($R^2 = 0.87$), $\delta D = 4.77\delta^{18}\text{O} - 6.04$ ($R^2 = 0.76$), and $\delta D = 4.90\delta^{18}\text{O} - 5.92$ ($R^2 = 0.84$), respectively. The slope values of 4.74, 4.77, and 4.90 for these water samples indicate potential evaporation of recharging water prior to infiltration (Gat 1996; Murad and Krishnamurthy, 2008). Notably, the δD - $\delta^{18}\text{O}$ relationships for different water samples showed similar slope and intercept values, especially in surface water and shallow

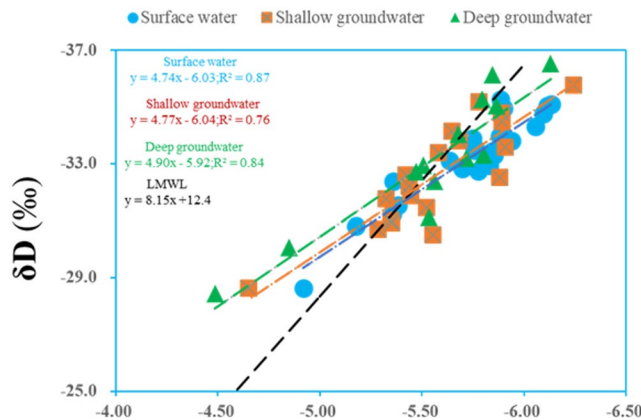


Fig. 3 Plots of $\delta^2\text{H}$ versus $\delta^{18}\text{O}$ of all water bodies

groundwater, suggesting that river water in the Lianjiang River watershed during the dry season was mainly recharged by adjacent groundwater.

Variation of fatty acids in surface water and groundwater

The mean concentrations of Σ -Fatty acid (Σ -Fatty acid denotes total quantified fatty acids (SFAs + MUFA + PUFA) in deep groundwater samples during the dry season were higher than those in surface water and shallow groundwater samples (Table 2). SFA was the primary component of fatty acids in all water samples, with PUFA contributing minimally to the total fatty acid concentrations. Furthermore, the large standard deviation values in SFA and Σ -Fatty acid indicate significant variation ($p < 0.05$), suggesting that different factors influenced the fatty acid concentrations in various water samples.

Source identification of fatty acids in shallow groundwater

As discussed above, concentrations of NO_3^- and SO_4^{2-} in shallow groundwater samples were higher than those in river water and deep groundwater, and river water was recharged by adjacent groundwater in dry season. Thus, we inferred that anthropogenic activities were affecting the fatty acids sources and behaviors in shallow groundwater. As the multivariate analytical tool, principal component analysis (PCA) is used to reduce a set of original variables

Table 2 Descriptive statistics of fatty acids in surface water and groundwater (ng/L)

Type	SFA ^a (ng/L)	MFA ^b	PUFA ^c	Σ -Fatty acids
Surface water ($n=11$)				
Min.	5596	51	4	3918
Max.	54,225	2113	213	54,900
Mean	14,960	545	90	15,595
SD	14,175	564	127	14,164
Shallow groundwater ($n=19$)				
Min.	6748	19	0	2389
Max.	34,102	2020	525	35,517
Mean	15,076	399	126	15,600
SD	9753	534	195	10,089
Deep groundwater ($n=11$)				
Min.	2578	91	8	2677
Max.	72,280	2029	788	75,697
Mean	26,367	729	258	27,353
SD	19,754	701	298	20,378

^a n-fatty acids are all straight-chained, saturated carboxylic acids

^b Monounsaturated fatty acids

^c Polyunsaturated fatty acids include all carboxylic acids with two or more double bonds

and to extract a small number of latent factors for analyzing relationships among the observed variables (Golobočanin et al. 2004). Accordingly, using Varimax normalized rotation, three principal components with eigenvalues >1 were extracted for fatty acids in shallow groundwater, accounting for 74.99% of total variance in dataset (Table S1).

As shown in Table 3, Factor 1 (27.49% variance explained) was primarily driven by saturated fatty acids (SFAs: C16:0, C18:0, C20:0-C30:0), monounsaturated fatty acids (MFAs: C18:1-trans-9), and polyunsaturated fatty

Table 3 The main calculated results of principal component analysis

Variables	Rotated component matrix		
	F1	F2	F3
C27:0	0.94	0.07	0.05
C29:0	0.91	0.15	0.17
C20:3-cis-8,11,14	0.90	0.07	0.28
C30:0	0.85	0.04	0.12
C22:6	0.84	0.24	0.06
C22:5-4,7,10,13,16	0.74	-0.10	0.07
C28:0	0.73	0.11	0.58
C18:0	0.72	0.11	0.48
C20:2-cis-11,14	0.72	0.09	0.49
C21:0	0.71	0.49	0.19
C16:0	0.70	0.16	0.15
C15:1	0.69	0.09	0.00
C20:0	0.67	0.31	0.65
C22:0	0.66	0.27	0.64
C18:1-trans-9	0.64	0.04	0.52
C26:0	0.62	0.03	0.49
C23:0	0.61	0.11	-0.04
C25:0	0.34	0.04	0.08
C13:0	-0.16	0.97	0.00
C14:0	0.02	0.94	0.01
C16:1	-0.13	0.93	0.22
C15:0	-0.05	0.91	0.37
C20:5-Cis-5,8,11,14,17	0.16	0.90	0.02
C18:3-Cis-6,9,12	0.26	0.84	0.32
C20:4-cis-5,8,11,14	0.32	0.82	0.17
C22:4	0.35	0.79	0.15
C22:5n3-7,10,13,16	0.36	0.76	0.09
C14:1	0.40	0.74	0.01
C12:0	0.08	0.66	-0.31
C18:2-Trans-9,12	0.06	0.66	0.65
C10:0	0.02	0.61	-0.48
C24:1	0.00	0.19	0.95
C22:1-Cis-13	-0.04	0.13	0.90
C20:1-Cis-11	0.32	0.02	0.86
C22:2-Cis-13,16	0.47	0.22	0.83
C24:0	0.52	0.15	0.81
C18:2-Cis-9,12	0.40	0.49	0.72
C17:0	0.53	0.38	0.67
C17:1	0.31	0.64	0.67
C8:0	0.01	0.28	-0.55
C11:0	0.00	0.50	-0.52
C6:0	-0.20	0.07	-0.36

acids (PUFAs: C20:2, C22:5, C20:3). While C16:0 and C18:0 co-occur in plankton and bacteria (McCallister et al. 2006; Wakeham 1985), MFA (C18:1 ω 9) and PUFA components exhibited bacterial signatures, collectively indicating natural FA inputs from soil organic matter (S-P Chang 1977).

Factor 2 (25.15% variance explained) featured medium-chain SFAs (C10:0-C15:0), MFAs (C14:1, C16:1, C17:1), and PUFAs (C18:2t, C22:5n3, C20:4, C18:3, C20:5). C15:0 originated from ruminant fats (Smedman 1999; Brevik et al. 2005), C16:1 was enriched in fish (Nair and Gopakumar 1978), C13:0/C17:1 represented ginkgolic acid pharmaceuticals (Ding et al. 2022), and C18:3/C20:4 (arachidonic acid) derived from botanical oils and animal tissues (Sergeant et al. 2016; Hanna and Hafez 2018), jointly characterizing pharmaceutical/cosmetic lipid inputs.

Factor 3 (22.36% variance explained) was dominated by long-chain SFAs (C17:0, C20:0-C24:0), MFAs (C17:1, C20:1, C22:1, C24:1), and PUFAs (C22:2, C18:2). C22:1 (erucic acid) served as a rapeseed oil biomarker (Jacobs 2011; Rabbani et al. 2017), C20:1 was enriched in Sapindaceae seed oils (Hopkins and Swingle 1967), and C17:0/C18:2 indicated ruminant fats and soybean oil (Jenkins et al. 2017; Gunawan et al., 2010), confirming fecal contamination sources.

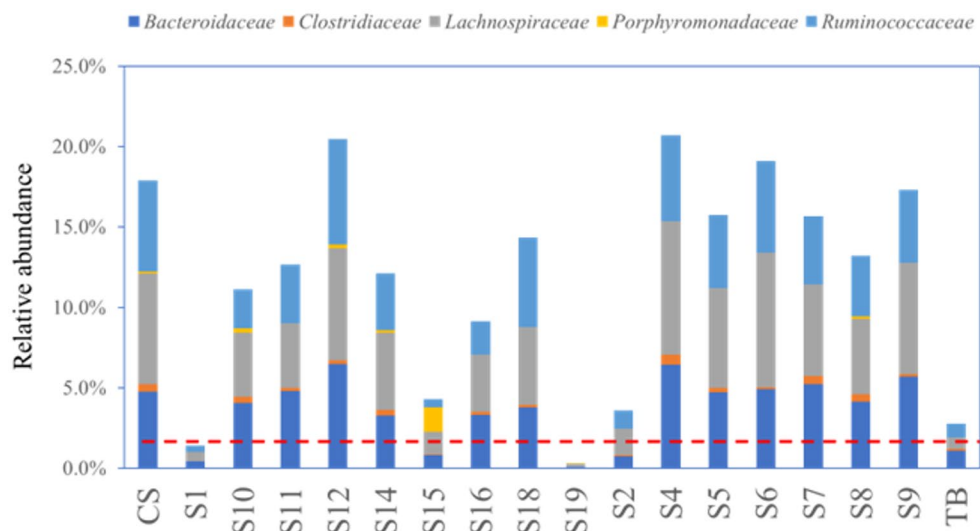
Generally, the sources of fatty acids in shallow groundwater can be broadly categorized into three groups: natural sources from soil organic matter (Rieley et al. 1991), anthropogenic sources from feces or domestic wastewater (Jenkins et al. 2017) and anthropogenic sources from pharmaceutical or cosmetic products present in domestic wastewater (Ding et al. 2022; Eini, 2002). Previous studies have identified and recognized fatty acids from surface soil organic matter, such as C26:0, C28:0, C30:0, and other typical PUFA (18:3 ω 3, 18:3 ω 6). However, the typical representative fatty acids from anthropogenic sources in groundwater remain unclear, and more evidence is needed to identify them.

Enhancing data interpretation using microbial data

Groundwater pollution identification using biological indicators

Previous studies suggest that feces-associated bacterial families, including *Bacteroidaceae*, *Porphyromonadaceae*, *Clostridiaceae*, *Lachnospiraceae*, and *Ruminococcaceae*, can serve as indicators of sewage and fecal contamination (Newton et al. 2013). When the relative contribution of these signatures exceeds 2% of the total microbial community, it suggests that the water may be affected by sewage and fecal contamination (Newton et al. 2013; Zhu et al. 2019). As depicted in Fig. 4, the sequences of these five families

Fig. 4 Bar plots of the relative abundance of sequences recovered and assigned to the fecal-associated bacterial families



typically represent 0.3%–20.7% of the total sequences in shallow groundwater. With the exception of sites ‘S1’ and ‘S19’, the relative contribution of sewage and fecal signatures at all other sites exceeded 2%, indicating that most groundwater samples were affected by manure and sewage.

Fecal-associated sources of fatty acid identification

Based on the PCA results in Sect. 3.3, factors 2 and 3 primarily indicate fatty acids that originate from sewage and fecal inputs in shallow groundwater. Therefore, we selected variables with coefficients > 0.8 in factors 2 and 3 as typical representative fatty acids to represent fatty acids from sewage and fecal inputs in shallow groundwater. The pharmaceutical or cosmetic sources of fatty acids include SFA (C13:0, C14:0, C15:0), MFA (C16:1), and PUFA (C20:5-Cis-5,8,11,14,17; C18:3-Cis-6,9,12, and C20:4-cis-5,8,11,14) in factor 2. The fecal-associated sources of fatty acids include SFA (C24:0), MFA (C22:1-Cis-13; C20:1-Cis-11), and PUFA (C24:1; C22:2-Cis-13,16) in factor 3.

To determine the specific sources of fatty acids in shallow groundwater between factor 2 and factor 3, we constructed a relationship between feces-associated bacterial families and the specific sources of fatty acids selected in factor 2 and factor 3. As shown in Fig. 5, a strong positive relationship was observed between feces-associated bacterial families and fecal-associated sources of fatty acids (Fig. 5b), while no significant relationship was found between feces-associated bacterial families and pharmaceutical or cosmetic sources of fatty acids (Fig. 5a). Thus, the typical representative fatty acids (C24:0; C22:1-Cis-13; C20:1-Cis-11; C24:1 and C22:2-Cis-13,16) in factor 3 are indicative of fecal-associated sources.

Surface water–groundwater relationship, and their influence on the occurrence of fatty acids

The water chemistry and stable isotopes (δD and $\delta^{18}\text{O}$) of surface water and groundwater in the Lianjiang river watershed indicated that the river water was recharged by adjacent groundwater, and that groundwater samples, particularly shallow groundwater, were impacted by human activities. Rapid infiltration via karst conduits facilitates downward transport of river-derived fatty acids, amplified by microbial solubilization (Zhu et al., 2020) and colloid-mediated mobility (Sun et al., 2021). Given the water environment characteristics and the relationship between surface water and groundwater, it is necessary to study the occurrence of fatty acids in karst watersheds. Based on the PCA results and microbial data interpretation, the sources of fatty acids in groundwater can be classified into three categories: ①Soil organic matter-associated source (C27:0+C29:0+C20:3-cis-8,11,14+C30:0+C22:6); ②Pharmaceutical or cosmetic-associated source (C13:0+C14:0+C16:1+C15:0+C20:5-Cis-5,8,11,14,17+C18:3-Cis-6,9,12+C20:4-cis-5,8,11,14); and ③Fecal-associated source (C24:1+C22:1-Cis-13+C20:1-Cis-11+C22:2-Cis-13,16+C24:0). 3.6.1. Spatial distribution characteristics of different sources of fatty acids.

Our study found that the concentrations of three different sources of fatty acids in deep groundwater were much higher than those in surface water and shallow groundwater, and that the concentrations of these fatty acids in shallow groundwater were the lowest. The concentrations of three different sources of fatty acids in surface water were similar to those in river water. Moreover, the concentration of pharmaceutical or cosmetic-associated source fatty acids was much higher than those of soil organic matter-associated and fecal-associated source fatty acids (Table 4).

Fig. 5 The relationship between feces-associated bacterial families (relative abundance) and fatty acids (Fig. 5a refers to the relationship between pharmaceutical or cosmetic-associated sources fatty acids and feces-associated bacterial families; Fig. 5b refers to the relationship between fecal-associated sources of fatty acids and feces-associated bacterial families)

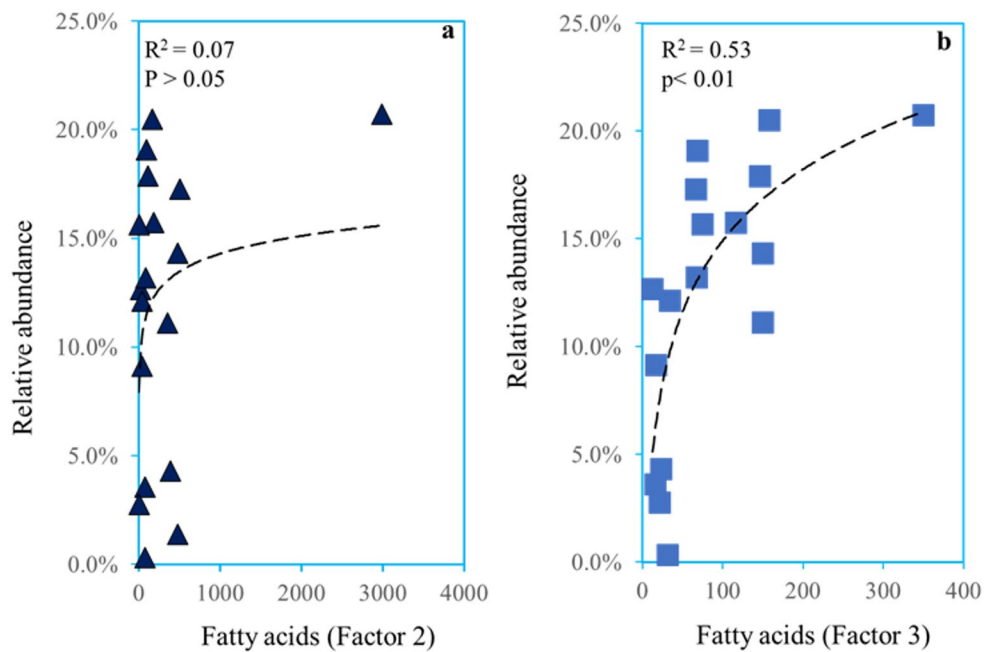


Table 4 Descriptive statistics of fatty acids in different water bodies (ng/L)

Item	River water	Shallow groundwater	Deep groundwater
A	Range 9.7–80.8	1.7–518.0	13.7–1535.0
	Median±SD 38.0±20.6	36.7±117.6	87.7±468.5
B	Range 44.6–3197.1.6.1	4.7–2943.3.7.3	1.7–1177.6.7.6
	Median±SD 160.6±955.4	106.1±662.7	683.3±769.2
C	Range 16.0–849.5.0.5	5.2–796.5.2.5	37.2–452.8.2.8
	Median±SD 76.9±238.0	62.9±179.1	105.5±156.4

SD Standard deviation

A: Soil organic matter-associated source fatty acids

B: Pharmaceutical or cosmetic-associated source fatty acids

C: Fecal-associated source fatty acids

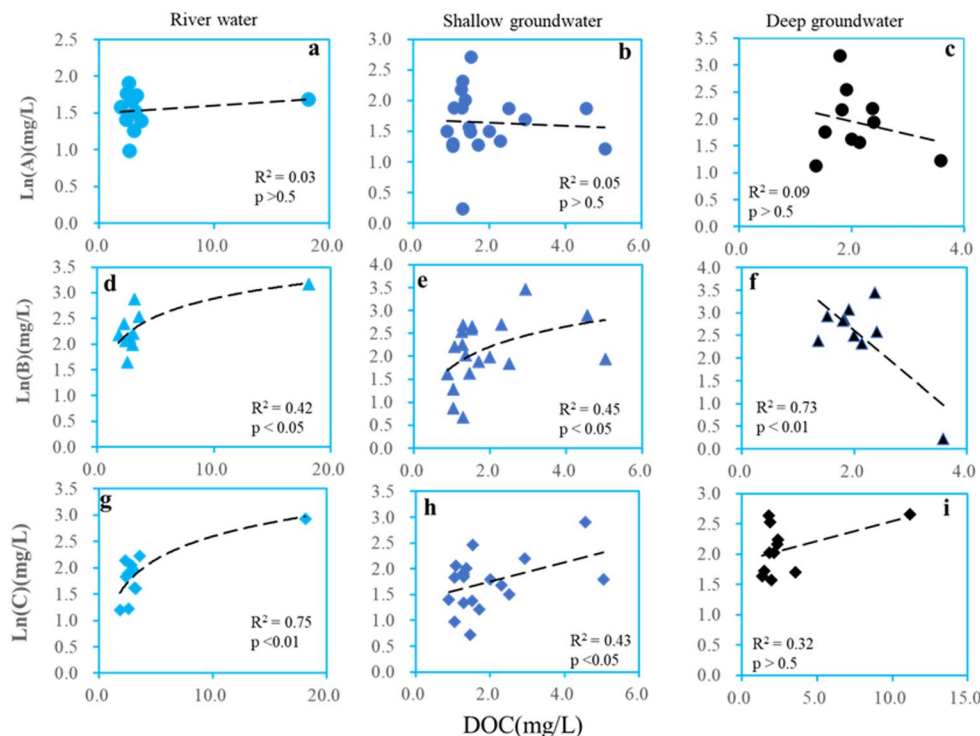
Our study found that the characteristics of the fatty acids in surface water (river water) were similar to those in groundwater, with pharmaceutical or cosmetic-associated source of fatty acids dominating, followed by soil organic matter-associated source of fatty acids. This suggests that the fatty acids in river waters may serve as sources of groundwater fatty acids. Additionally, a strong positive relationship was observed between DOC concentrations and the concentrations of pharmaceutical or cosmetic-associated source of fatty acids ($p < 0.05$), as well as the concentrations of fecal-associated source of fatty acids ($p < 0.05$) in both surface water and shallow groundwater (Fig. 6e, d, and h). However, no significant relationship was found between the concentrations of soil organic matter-associated source of fatty acids and DOC concentrations in both river water and shallow groundwater (Fig. 6a and b).

In the study area, soil organic matter-associated source of fatty acids is not the primary contributor to the natural sources of fatty acids in surface water (river water). This is because autochthonous sources of fatty acids in groundwater, including plankton, algae, macrophytes, and bacteria in river water, also play a significant role in contributing to fatty acids. Therefore, soil organic matter-associated source of fatty acids cannot represent the entirety of natural sources of fatty acids in river water. Additionally, during the dry season when agricultural activities are minimal and precipitation is scarce, river water is less affected by non-point source pollution. As a result, anthropogenic sources of fatty acids through groundwater recharge, specifically pharmaceutical or cosmetic-associated source and fecal-associated source, are the primary sources of fatty acids in river water. Interestingly, no significant positive relationships were observed between the concentrations of fatty acids and DOC in deep groundwater (Fig. 6e, f, and i). This suggests that allochthonous sources (soil organic matter-associated sources) and anthropogenic sources of organic matter (pharmaceutical or cosmetic-associated source & fecal-associated source) contribute little to the total organic matter concentrations in deep groundwater. However, the concentration of fatty acids in deep groundwater was higher than those in shallow groundwater and river water, indicating that the deep karst aquifer may act as an organic matter sink during the dry season.

Conclusions

This study aimed to assess the concentration and spatial variations of fatty acids, determine their sources in shallow groundwater, and investigate the impact of the

Fig. 6 Relationship of fatty acids concentrations and DOC concentrations in different water bodies (Fig. 6a, b, and c represent the relationship between soil organic matter-associated source of fatty acids concentrations and DOC concentrations in river water, shallow ground water and deep groundwater, respectively; Fig. 6d, e, and f represent the relationship between pharmaceutical or cosmetic-associated source of fatty acids concentrations and DOC concentrations in river water, shallow ground water and deep groundwater, respectively; Fig. 6g, h, and i represent the relationship between fecal-associated source of fatty acids concentrations and DOC concentrations in river water, shallow ground water and deep groundwater, respectively)



surface-groundwater relationship on fatty acids distribution in the Lianjiang river watershed. The main conclusions of this study are as follows: Fatty acids concentrations in shallow groundwater were similar to those in river water, while fatty acid concentrations in deep groundwater were highest during the dry season. Fatty acids in shallow groundwater were classified into two main sources: natural sources (soil organic matter sources) and anthropogenic sources (pharmaceutical or cosmetic-associated source & fecal-associated source) based on PCA statistical methods and microbial data. There was a significant positive correlation ($R^2=0.53$ for quadratic fit) between anthropogenic sources of fatty acids in river water and shallow groundwater, which explains the consistent anthropogenic sources of fatty acids in both river water and deep groundwater. Hydrochemistry and stable isotopes evidence showed that river water was recharged by adjacent groundwater and was influenced by the relationship between river water and shallow groundwater, which affected the spatial distribution of anthropogenic sources of fatty acids. The deep karst aquifer may serve as an organic matter sink in the karst watershed due to its unique structural characteristics. In summary, findings from this study have shown the importance of the interaction between river and groundwater and their implications for the potential DOM behavior in karst river basin. However, further studies should be carried out to fully understand the potential DOM behavior in karst river basin.

Supplementary Information The online version contains supplementary material available at <https://doi.org/10.1007/s12665-025-12647-w>.

Author contributions Zuobing Liang and Shaoheng Li contributed to formal statistical analysis, writing and reviewing of the manuscript; Rui Li contributed to methodology and reviewing of the manuscript; Qirui Wu performed element concentrations analysis and reviewing of the manuscript; Zaizhi Yang contributed to methodology and reviewing of the manuscript; Di Tian contributed to methodology; Pengcheng Zhang, Kun Ren and Lei Gao: analyzing or interpreting the data; Jianyao Chen: contributed writing and reviewing of the manuscript.

Funding This work was financially supported by National Natural Science Foundation of China (42302269), the Guangxi Natural Science Foundation [2023JJD150024], and Special Fund for Basic Scientific Research of Institute of Karst Geology, CAGS [2023018].

Data availability Data will be made available on request.

Declarations

Competing interests The authors declare no competing interests.

References

- Bernhardt ES, Likens GE (2002) Dissolved organic carbon enrichment alters nitrogen dynamics in a forest stream. *Ecology* 83(6):1689–1700. [https://doi.org/10.1890/0012-9658\(2002\)083\[1689:DOCEAN\]2.0.CO;2](https://doi.org/10.1890/0012-9658(2002)083[1689:DOCEAN]2.0.CO;2)
- Borović S, Terzić J, Pola M (2019) Groundwater quality on the Adriatic karst Island of Mljet (Croatia) and its implications on water supply. *Geofluids* 2019:5142712. <https://doi.org/10.1155/2019/5142712>
- Brevik et al (2005) Evaluation of the odd fatty acids 15:0 and 17:0 in serum and adipose tissue as markers of intake of milk and dairy fat. *Eur J Clin Nutr* 59(12):1417–1422. <https://doi.org/10.1038/sj.ejcn.1602256>

Busico G (2020) A novel hybrid method of specific vulnerability to anthropogenic pollution using multivariate statistical and regression analyses. *Water Res* 171:115386. <https://doi.org/10.1016/j.watres.2019.115386>

Chang S-P, Rothfus JA (1977) Enrichment of eicosenoic and docosadienoic acids from *limnanthes* oil. *J Am Oil Chem Soc* 54(11):549–552. <https://doi.org/10.1007/BF02909080>

Charlier et al (2012) Conceptual hydrogeological model of flow and transport of dissolved organic carbon in a small Jura karst system. *J Hydrol* 460:52–64. <https://doi.org/10.1016/j.jhydrol.2012.06.043>

Christodoulou et al (2009) Use of lipids and their degradation products as biomarkers for carbon cycling in the Northwestern mediterranean sea. *Mar Chem* 113(1):25–40. <https://doi.org/10.1016/j.marchem.2008.11.003>

Cory RM, McKnight DM (2005) Fluorescence spectroscopy reveals ubiquitous presence of oxidized and reduced quinones in dissolved organic matter. *Environ Sci Technol* 39(21):8142–8149. <https://doi.org/10.1021/es0506962>

Ding et al (2022) Pharmacological activities of ginkgolic acids in relation to autophagy. *Pharmaceuticals (Basel Switzerland)* 15(12). <https://doi.org/10.3390/ph15121469>

Eini, Tamarkin (2002) Pharmaceutical and cosmetic carrier or composition for topical application, edited, EINI MEIR

Gat JR (1996) Oxygen and hydrogen isotopes in the hydrologic cycle. *Annu Rev Earth Planet Sci* 24(1):225–262. <https://doi.org/10.1146/annurev.earth.24.1.225>

Golbočanin et al (2004) Principal component analysis for soil contamination with PAHs. *Chemometr Intell Lab Syst* 72(2):219–223. <https://doi.org/10.1016/j.chemolab.2004.01.017>

Green SM et al (2019) Soil functions and ecosystem services research in the Chinese karst critical zone. *Chem Geol* 527:119107. <https://doi.org/10.1016/j.chemgeo.2019.03.018>

Gunawan, Ju (2010) Analysis of trans–cis fatty acids in fatty acid Steryl esters isolated from soybean oil deodoriser distillate. *Food Chem* 121(3):752–757. <https://doi.org/10.1016/j.foodchem.2009.12.079>

Hanna, Hafez (2018) Synopsis of arachidonic acid metabolism: A review. *J Adv Res* 11:23–32. <https://doi.org/10.1016/j.jare.2018.03.005>

Hartmann (2014) Karst water resources in a changing world: review of hydrological modeling approaches. *Rev Geophys* 52(3):218–242. <https://doi.org/10.1002/2013RG000443>

Hopkins, Swingle (1967) Eicosenoic acid and other fatty acids Of Sapindaceae seed oils. *Lipids* 2(3):258–260. <https://doi.org/10.1007/BF02532565>

Jacobs et al (2011) Effects of feeding rapeseed oil, soybean oil, or linseed oil on stearoyl-CoA desaturase expression in the mammary gland of dairy cows. *J Dairy Sci* 94(2):874–887. <https://doi.org/10.3168/jds.2010-3511>

Jaffé et al (2008) Spatial and Temporal variations in DOM composition in ecosystems: the importance of long-term monitoring of optical properties. *J Geophys Research: Biogeosciences* 113(G4). <https://doi.org/10.1029/2008JG000683>

Jenkins et al (2017) Odd chain fatty Acids; new insights of the relationship between the gut Microbiota, dietary Intake, biosynthesis and glucose intolerance. *Sci Rep* 7(1):44845. <https://doi.org/10.1038/srep44845>

Jin et al (2012) Determination of nitrate contamination sources using isotopic and chemical indicators in an agricultural region in China. *Agric Ecosyst Environ* 155:78–86. <https://doi.org/10.1016/j.agee.2012.03.017>

Jin et al (2014) Organic and inorganic carbon dynamics in a karst aquifer: Santa Fe river Sink-Rise system, North Florida, USA. *J Geophys Research: Biogeosciences* 119(3):340–357. <https://doi.org/10.1002/2013JG002350>

Li et al (2017) PAHs behavior in surface water and groundwater of the yellow river estuary: evidence from isotopes and hydrochemistry. *Chemosphere* 178:143–153. <https://doi.org/10.1016/j.chemosphere.2017.03.052>

Li et al (2019) Isotopic and geochemical interpretation of groundwater under the influences of anthropogenic activities. *J Hydrol* 576:685–697. <https://doi.org/10.1016/j.jhydrol.2019.06.037>

Liang (2018) Identification of the dominant hydrogeochemical processes and characterization of potential contaminants in groundwater in Qingyuan, China, by multivariate statistical analysis. *RSC Adv* 8(58):33243–33255. <https://doi.org/10.1039/c8ra06051g>

Liu et al (2018a) FDOM conversion in karst watersheds expressed by Three-Dimensional fluorescence spectroscopy. *Water* 10(10):1427

Liu et al (2018b) FDOM conversion in karst watersheds expressed by Three-Dimensional fluorescence spectroscopy. *Water* 10(10). <https://doi.org/10.3390/w10101427>

Lü et al (2020) Characteristics and influencing factors of hydrochemistry and dissolved organic matter in typical karst water system. *Environ Sci Pollut Res* 27(10):11174–11183. <https://doi.org/10.1007/s11356-019-07227-y>

McCallister et al (2006) Sources of estuarine dissolved and particulate organic matter: A multi-tracer approach. *Org Geochem* 37(4):454–468. <https://doi.org/10.1016/j.orggeochem.2005.12.005>

Medici et al (2021) DOC and nitrate fluxes from farmland; impact on a dolostone aquifer KCZ. *J Hydrol* 595:125658. <https://doi.org/10.1016/j.jhydrol.2020.125658>

Nair Gopakumar (1978) Fatty acid compositions of 15 species of fish from tropical waters. *J Food Sci* 43(4):1162–1164. <https://doi.org/10.1111/j.1365-2621.1978.tb15260.x>

Napolitano et al (1997) Fatty acids as trophic markers of phytoplankton blooms in the Bahía Blanca estuary (Buenos Aires, Argentina) and in trinity Bay (Newfoundland, Canada). *Biochem Syst Ecol* 25(8):739–755. [https://doi.org/10.1016/S0305-1978\(97\)00053-7](https://doi.org/10.1016/S0305-1978(97)00053-7)

Newton et al (2013) A microbial signature approach to identify fecal pollution in the waters off an urbanized Coast of lake Michigan. *Microb Ecol* 65(4):1011–1023. <https://doi.org/10.1007/s00248-013-0200-9>

Quiers et al (2014) Characterisation of rapid infiltration flows and vulnerability in a karst aquifer using a decomposed fluorescence signal of dissolved organic matter. *Environ Earth Sci* 71(2):553–561. <https://doi.org/10.1007/s12665-013-2731-2>

Rabbani et al (2017) Binding of erucic acid with human serum albumin using a spectroscopic and molecular Docking study. *Int J Biol Macromol* 105:1572–1580. <https://doi.org/10.1016/j.ijbiomac.2017.04.051>

Riley et al (1991) Sources of sedimentary lipids deduced from stable carbon-isotope analyses of individual compounds. *Nature* 352(6334):425–427. <https://doi.org/10.1038/352425a0>

Rielley G, Collier RJ, Jones DM, Eglinton G (1991) The biogeochemistry of Ellesmere Lake, U.K.—I: source correlation of leaf wax inputs to the sedimentary lipid record. *Org Geochem* 17:901–912. [https://doi.org/10.1016/0146-6380\(91\)90031-E](https://doi.org/10.1016/0146-6380(91)90031-E)

Sergeant et al (2016) Gamma-linolenic acid, Dihommo-gamma linolenic, eicosanoids and inflammatory processes. *Eur J Pharmacol* 785:77–86. <https://doi.org/10.1016/j.ejphar.2016.04.020>

Simon et al (2010) Spatial and Temporal patterns in abundance and character of dissolved organic matter in two karst aquifers. *Fundamental Appl Limnol* 177(2):81–92. <https://doi.org/10.1127/1863-9135/2010/0177-0081>

Smedman et al (1999) Pentadecanoic acid in serum as a marker for intake of milk fat: relations between intake of milk fat and metabolic risk factors. *Am J Clin Nutr* 69(1):22–29. <https://doi.org/10.1093/ajcn/69.1.22>

Sullivan et al (2019) Nitrate transport in a karst aquifer: numerical model development and source evaluation. *J Hydrol* 573:432–448. <https://doi.org/10.1016/j.jhydrol.2019.03.078>

Sun., (2021) Speciation, distribution and migration pathways of polycyclic aromatic hydrocarbons in a typical underground river system in Southwest China. *J Hydrol*, 596, 125690, <https://doi.org/10.1016/j.jhydrol.2020.125690>

Wakeham SG (1985) Wax esters and triacylglycerols in sinking particulate matter in the Peru upwelling area (15°S, 75°W). *Mar Chem* 17(3):213–235. [https://doi.org/10.1016/0304-4203\(85\)90012-X](https://doi.org/10.1016/0304-4203(85)90012-X)

Worthington et al (2012) Effective porosity of a carbonate aquifer with bacterial contamination: Walkerton, Ontario, Canada. *J Hydrol* 464–465:517–527. <https://doi.org/10.1016/j.jhydrol.2012.07.046>

Yao et al (2014) Dissolved organic matter (DOM) dynamics in karst aquifer systems. *Huanjing Kexue* 35(5):1766–1772

Yoshinaga MY, Sumida PYG, Wakeham SG (2008) Lipid biomarkers in surface sediments from an unusual coastal upwelling area from the SW Atlantic ocean. *Org Geochem* 39(10):1385–1399. <https://doi.org/10.1016/j.orggeochem.2008.07.006>

Željković Kadić (2015) Groundwater balance estimation in karst by using simple conceptual rainfall–runoff model. *Environ Earth Sci* 74:6001–6015

Zhu. (2020) Integrating hydrochemical and biological approaches to investigate the surface water and groundwater interactions in the hyporheic zone of the Liuxi river basin, Southern China. *J Hydrol* 583:124622. <https://doi.org/10.1016/j.jhydrol.2020.124622>

Zhu et al (2019) Combined microbial and isotopic signature approach to identify nitrate sources and transformation processes in groundwater. *Chemosphere* 228:721–734. <https://doi.org/10.1016/j.chemosphere.2019.04.163>

Publisher's note Springer Nature remains neutral with regard to jurisdictional claims in published maps and institutional affiliations.

Springer Nature or its licensor (e.g. a society or other partner) holds exclusive rights to this article under a publishing agreement with the author(s) or other rightsholder(s); author self-archiving of the accepted manuscript version of this article is solely governed by the terms of such publishing agreement and applicable law.